Experimental studies on evaporation kinetics of gold nanofluid droplets: Influence of nanoparticle sizes and coating on thermal performance

Ibrahim Zaaroura, Souad Harmand, Julien Carlier, Malika Toubal, Aurélie Fasquelle, Bertrand Nongaillard

Experimental studies on evaporation kinetics of gold nanofluid droplets: Influence of nanoparticle sizes and coating on thermal performance

Ibrahim Zaaroura *[a, b], Souad Harmand*[a], Julien Carlier [b], Malika Toubal [b], Aurélie Fasquelle [c] Bertrand Nongaillard [b]

a- Univ. Polytechnique Hauts-de-France, CNRS, UMR 2201- LAMIH - Laboratoire d'Automatique de Mécanique et d'Informatique Industrielles et Humaines, F-59313 Valenciennes, France

b- Univ. Polytechnique Hauts-de-France, CNRS, Univ. Lille, YNCREA, Centrale Lille, UMR 8520 - IEMN -DOAE, F-59313 Valenciennes, France

c- Jeumont Electric, 59460 Jeumont, France

Abstract

In this work, a series of experiments investigate the evaporation of gold nanofluid sessile droplets on a perfluorodecyltrichlorosilane (PFTS) silicon substrate heated to 77 °C. The evaporation processes of different nanofluid droplets of the same initial volume, all for a 1% C_v volume concentration prepared from the 0.1mM original suspension, are visualized to examine the size effect of gold nanoparticles (2.2, 5 and 10 nm) and the impact of surface coating (with and without Citrate capping in phosphate-buffered saline solvent) on enhancing heat transfer. This study open access to understand the size effect of gold nanoparticle in very small scale and the different types of surfactant on heat and mass transfer during the evaporation of droplet. Two methods are used to analyze the evaporation process, an optical one coupled to an infrared thermography method and an acoustic method. These complementary methods have the ability to investigate clearly the solid/liquid and liquid/vapor interfaces at the same time. From the optical observation, using a Drop Shape Analyzer (Kruss system), the evolution in time of the shape of the droplets (contact angle, base diameter and volume) are measured under controlled conditions (Humidity=50%, T_{atm}=23°C). Then, the evaporation rate is deduced from the measurements of the evolution of volume in time. At the same time, an infrared camera is used to observe the droplet surface gradient temperature, air/liquid interface, due to thermal Marangoni flow. The acoustic method, based on a high- frequency echography principle, allowed to monitor the stability of nanoparticles inside the droplets (Au-water mixture) during the process of evaporation. From the kinetics of the reflection coefficient at the interface of the silicon substrate over which the nanofluids are deposited, the results show that the evaporation rate of 5 nm Au-water mixture (phosphate buffered saline solvent only) was faster than that of 10 nm Au-water mixture. While with citrate capping-PBS, the evaporation rate of the largest particle sizes (10 nm Au-water mixture) was the fastest than that of the smaller sizes (2.2 and 5 nm). Also, the 5 nm gold nanofluids with PBS showed the highest evaporation rate (+35%) than that of citrate capping gold nanofluids (+15%). As results, the addition of a surfactant (citrate capping) decreases the effectiveness of the heat transfer of gold nanofluids. This seems to be due to the absence of Marangoni cells in droplets made of Au-water mixtures (Citrate capping-PBS). Moreover, reducing in the thermal conductivity of gold nanofluid due to the surfactant coating by covering the gold nanoparticles surface and this eventually affected the nanofluid thermal

properties. This is further supported by the acoustic method, which clearly shows worse stability of the nanoparticles in the latter case.

Keywords: gold nanoparticles; surfactant; marangoni cells; evaporation rate; droplets evaporation.

List of Symbols

%C*v*	Volume Concentration, %
$\lvert R \rvert$	Modulus of the reflection Coefficient
R_{LL}	Longitudinal Waves
H	Humidity, %
T_{atm}	Atmospheric Temperature, °C
DSA	Drop shape Analyzer
Au	Gold Nanoparticles
PBS	Phosphate-Buffered Saline
PFTS	Perfluorodecyltrichlorosilane
V*i*	Initial Volume

Introduction

A heat transfer fluid is a fluid medium used in a system for adding to or removing from the system an amount of heat at an adequate rate to ensure the functionality and reliability of the system. For that reason, new nanotechnology is used to enhance and improve the heat transfer in these systems such as Electronic cooling systems, Heat pipes, Nuclear reactors, and so on [1-4]. This nanotechnology is known as Nanofluids where nanoparticles, in nano sizes, are suspended in base fluids (water, minerals oil, binary mixtures) [5-7]. These nanoparticles have the advantage of improving the heat transfer by absorbing rapidly the excess heat and transmit it outside the system. This improvement is due to their thermophysical properties that showed special advantages, such as better stability, greater thermal conductivity, and lower pressure drop [8-11]. However, the use of nanofluids substantially depends not only on thermal conductivity but also on their viscosity. Viscosity indeed has a negative effect on the enhancement of heat transfer. [12, 13]

Many studies were done to analyze the effect of different types of nanoparticles, such as copper oxide, graphene oxide, and carbon nanotubes on the efficiency of heat transfer [14-16]. Also, the effect of nanoparticle sizes (in nanoscale) on heat transfer with different average diameters (1 nm to 100nm) [17]. Some studies show the enhancement in the coefficient of heat transfer by 25% as we increase the size of nanoparticles whereas others showed the inverse [18, 19]. So, this variation is due to the type of nanoparticles used. Moreover, the influence of nanoparticle coating and their chemical preparation have also its effect on the performances of heat transfer. These chemical preparation presented by coating the nanoparticles with surfactant is used to stabilize the nanoparticles inside the fluids and to avoid the agglomeration or sedimentation in the system.

Nanofluid droplet evaporation has gained many audience nowadays due to its very important phenomenon and wide applications in fuel and sprays cooling [20, 21]. Many researchers work on the drying progress and deposition formation from the evaporative sessile droplets with the suspended insoluble solutes, especially nanoparticles [22-25]. The main content covers the evaporation fundamental, the particle self-assembly, and kinetic deposition of nanoparticles in a sessile nanofluid droplet. The effects of the surfactant and size of nanoparticles on the evaporative dynamics are elucidated at first and the deposition process which is introduced

afterward. Droplet shape, spreading dynamics, evaporation rate, and evaporation regimes are the factors affected by the addition of particles.

Droplets evaporate on surfaces and measured using digital image technique (Kruss System) and with this technique we are able to measure the droplet profile, volume, contact angle, base diameter, and droplet height in time-dependent [26,27]. So, with this method, we are able to select directly the better nanoparticles to use later in heat exchanger systems. Many factors play an important role in the enhancement of nanofluids droplet evaporation such as Marangoni convection cells and their stability with the base fluid. Nanoparticles have an effect on Marangoni flow, which causes a capillary flow outward from the center of the drop brings suspended particles to the drop edge as the evaporation process. Hu et al. [28] showed that Marangoni flow reversed the coffee-ring phenomenon and produces deposition at the droplet center rather than the edge. Also, in his other research work [29] Hu et al. explained the effects of Marangoni on the evaporating sessile droplet.

Thus, the edge or droplet contact line has the highest evaporation as it's a weak zone. [30] Nanoparticles deposition has a direct effect on heat and mass transfer since the deposition of nanoparticles loses their effectiveness inside the fluid by absorbing the excess heat and transfer it outside and this led to increasing in the system thermal resistance. So, it is very important to takes into account all the conditions for a better thermal system.

In this study, experiments on the evaporation of nanofluids sessile droplets on heated hydrophobic surfaces are conducted using optical and infrared measurements. The objective of this work is to:

- Study the effect of gold nanoparticle with very interesting small sizes (2.2, 5 and 10 nm).
- The effect of surfactant represented by citrate coating and PBS as reactant free on the droplet evaporation rate of heat transfer.
- Introducing a new method illustrated by acoustic high-frequency waves to give more important details at the solid/liquid interface.

2. Experimental setup

In this work, the studied nanofluid consists of gold (Au) nanoparticles (Sigma Aldrich, Molecular weight = 196.97 g/mol with a volume concentration of 1% C_v) dissolved in distilled

water (as a base fluid) and stabilized through ultrasonication (Elma, S 10/H) for at least 30 min before use. Three sizes of gold nanoparticles particle were used at 2.2, 5, and 10 nm for the citrate-capped PBS solution while 5 and 10 nm for the 0.1mM PBS, reactant free, **Table. 1**. PBS reactant free solution is used to stabilize the nanoparticle and to prevent any change in the PH of the gold nanofluid solution presented in volume concentration (See **Fig. 1**).

Figure 1. Gold nanofluids of different particle sizes and surfactants coating (PBS and PBS-citrate)

Nanoparticle, 1% C_v	Size (nm)	Buffer solutions	
Gold, Au	2.2	citrate-capped-PBS solution	-
Gold, Au	5	citrate-capped-PBS solution	0.1mM PBS, reactant free
Gold, Au	10	citrate-capped-PBS solution	0.1mM PBS, reactant free

Table 1. Properties of prepared nanofluids

To analyze the droplet evaporation process, two different methods are used, one using optical and infrared thermography measurements and the other one using acoustic reflection coefficient measurements at room temperature.

Nanofluids droplets are deposited, in both methods, on a silicon substrate modified with a perfluorodecyltrichlorosilane (PFTS) layer to achieve hydrophobic surfaces [31]. So, in that case, both methods have the same substrate characteristics. The optical measurements were achieved by increasing the temperature substrate from ambient to 77 °C. The calibration for the silicon

substrate emissivity calibration was done using the emissivity calculator by the infrared camera. The technique is to measure the surface temperature of a known emissivity material such as a black object attached to the silicon substrate. Form the known real temperature of the black object we can find the emissivity of the silicon substrate. This technique is suitable to find out the wanted substrate surface temperature. Finally, the water droplet analysis will be extracted with its known emissivity (≈0.97).

2.1. Infrared and optical measurements

This experimental setup allows us to calculate the evaporation rate of nanofluids droplets for each particle size and to visualize the convection cells caused due to Marangoni effect at high temperatures.

The substrate is heated using a joule effect by a resistance wire connected to the voltage supplier to control the temperature, **Fig 2**. The substrate is placed above a semiconductor material to homogenize the heating medium. Calibration was performed after adjusting the voltage setting for each surface temperature. The evaporation process of droplets is observed and recorded using high-speed camera from the side view (CCD camera, Allied Vision Technologies, 780 x 580 pixels) which connected to backlight lighting. Then a Kruss Drop Shape analyzer is used to measure the droplets profile (Contact Angle, Volume, Base diameter, etc...). At the same time, an infrared camera (FLIR, X6580SC, 640 x512 Pixels, 15 um detector pitch) is installed on the top for the infrared thermal mapping and visualization of thermal instabilities on the surface of the droplets through a sapphire window. The evaporation process was carried out under the same conditions (Initial volume droplet V_i =1.5 µL, Substrate surface temperature: Amb to 77 °C) inside a controlled chamber (H=50%, T_{atm}=23°C).

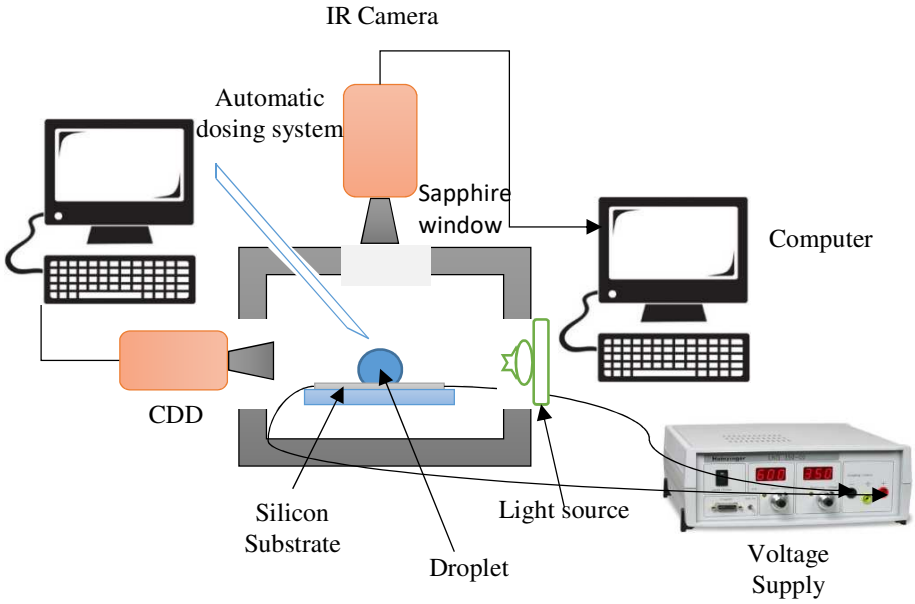

Figure 2. Schema of the experimental setup

2.2. Acoustic measurements

Measurements are made under a controlled atmosphere using an air-conditioning system. A Cascade PM8 prober system is used to control the position of the S/G (signal/ground) probe at the microscale level on a piezoelectric transducer as small as 250 µm in diameter to achieve electrical measurements, **Fig. 3**. The specificity of the probe is the possibility to achieve an electrical contact at the backside of the wafer on which the piezoelectric transducer was fabricated [32]. These probes are connected to a Rhode & Schwarz ZVA8 Vector Network Analyzer from which the modulus of the longitudinal reflection coefficient is deduced. The droplet is deposited on the top side of the silicon substrate via a microfluidic device, then a high-frequency (1 GHz) longitudinal wave is generated by ZnO piezoelectric transducers fabricated on the backside of the classical (100) crystal orientation of the silicon substrate on which the solid-liquid interface is characterized. The diameter of the ZnO transducers is about 250 µm. During the droplet evaporation, the modulus of the longitudinal reflection coefficient is modified as the particles settle. This method allows a highly sensitive analysis of what occurs at the liquid-solid interface. The study and analysis mechanism is similar to our work in Zaaroura et al. [27].

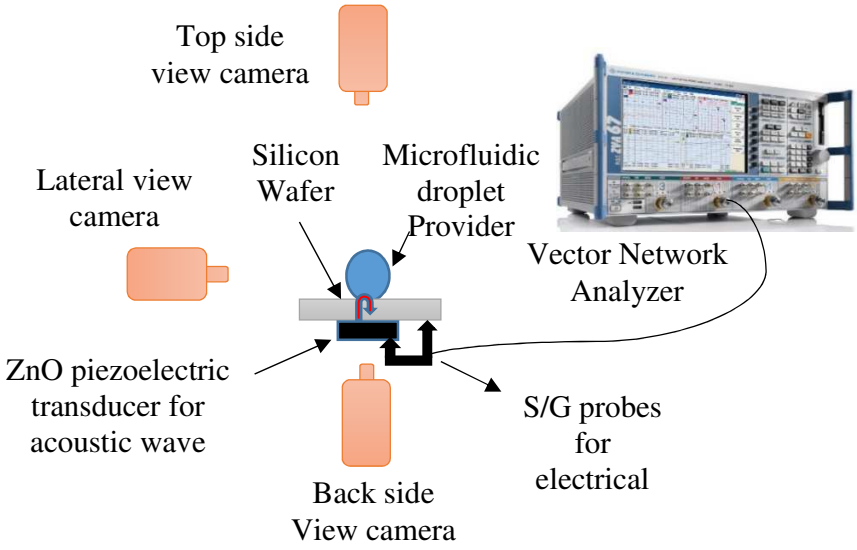

Figure 1. Schema of the experimental setup of acoustic measurements

3. Experimental Results

3.1. Infrared and optical investigations

The optical and infrared techniques are applied to investigate the dynamic evaporation of droplets of gold nanofluid. The CCD camera records the evaporation process and then the software Kruss Drop Shape Analyzer analyzes the profile of droplets and the evolution of droplets, contact angle, volume, and diameter, are accessible. Moreover, the infrared camera records the evaporation process at the top view and provides the gradient temperature distribution on the surface of the droplets.

3.1.1. Au nanofluid (1% C_v; 0.1mM PBS, reactant free) – Water Mixture, Particle Size Effects

For the water-Au mixture of different particle sizes (5, 10 nm), the result was compared to that of pure water on the $V^{2/3}$ plot. **Fig. 4** shows the evolution of $V^{2/3}$ for droplets of pure water and 1% C_v Au-water mixture of different particle sizes at different surface temperatures. While the measured contact angle with the silicon substrate showed the same starting value for all the mixtures, **Fig. 5**.

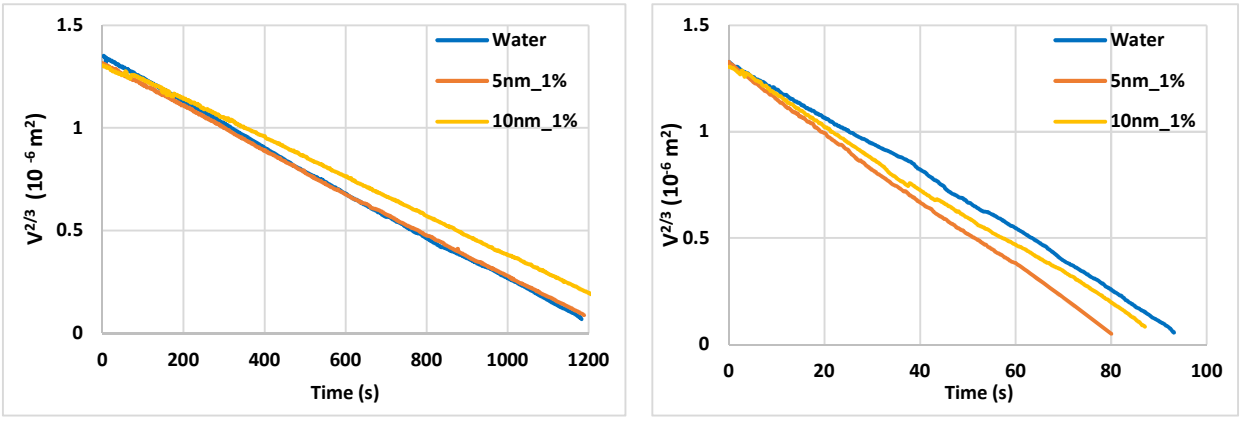

(a)

(b)

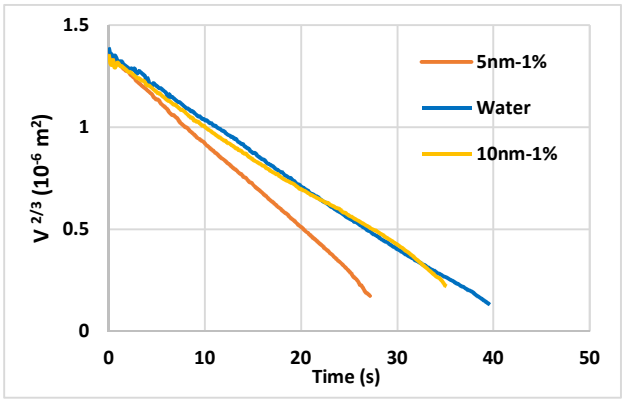

(c)

Figure 4. Evolutions of the volume for water and gold nanofluid, with different particle sizes under substrate temperatures (a) at ambient, (b) 55 °C and (c) 77 °C, versus time.

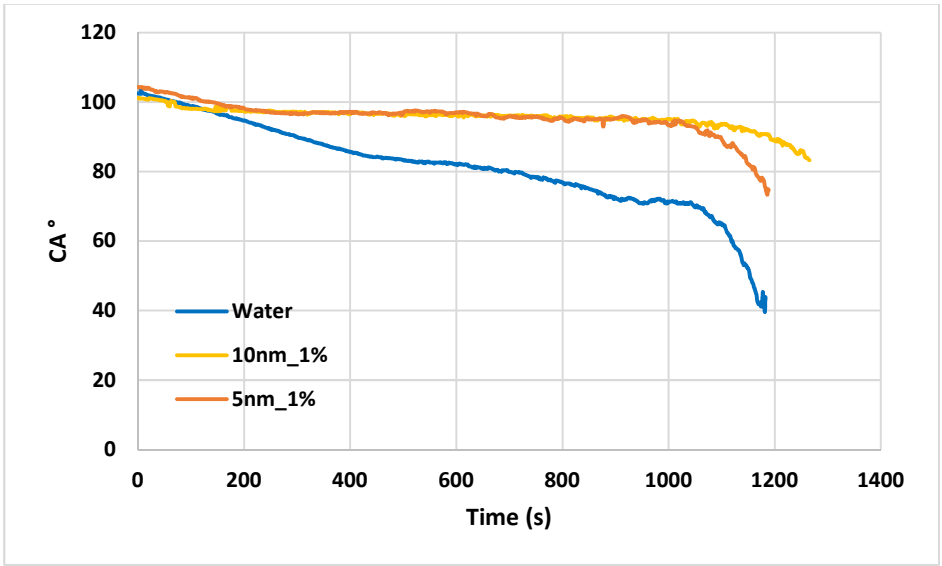

Figure 5. Normalized contact angle for water and gold nanofluids during evaporation, with different sizes (5 and 10 nm), at ambient temperature.

The results showed that at ambient temperature, the evaporation of pure water droplets was faster than the gold nanofluids of the two different sizes. Since reducing the contact angle increase the contact area between the droplet and solid surface and also reduces droplet thickness [33]. As the liquid layer becomes thinner, heat transfer from the solid to the liquid-vapor interface is enhanced. Both effects increases the droplet evaporation rate. The measured contact angle of pure water showed a decrease in its values more than that of droplet gold nanofluid and this validates the enhancement in its droplet evaporation.

When the surface temperature increased to 55 °C, the evaporation process showed a higher evaporation rate of the 5 nm Gold-water mixture with 17% while 3% for the 10 nm Gold-water mixture.

Similarly, at a surface temperature of 77 °C, the evaporation process showed a higher evaporation rate of the 5 nm Gold-water mixture with 35% whereas 2% for the 10 nm Gold-water mixture. Thus, the evaporation rate is found to depend on the size of the nanoparticles, which showed that the smallest particle size (5nm) has the greatest effect on increasing the evaporation proceeds during the droplet lifetime than the 10 nm.

This difference can be linked to different reasons, the effective surface area of 5 nm Au-water mixture is greater than the 10 nm Au-water by a factor 2 and this means a greater amount of water molecules can come into contact with a larger surface surrounding the 5nm nanoparticles, thus affecting reactivity). Furthermore, Infrared Camera images made it possible to detect the convection cells, **Fig. 6,** due to the Marangoni effect that appeared on the surface of droplets. These convection cells have the ability to increase the vapor mass transfer at the liquid-air interfaces and to induce a faster evaporation rate [34]. The convection cells created by the thermal Marangoni can be observed on the surface of the droplets when the substrate is heated to high temperatures. The convection cells of the gold nanofluids appeared and remained longer than those of pure water and this is due to the Brownian motion of nanoparticles inside the droplet. The absorption by solid particles of gold and their flow has the ability to stay longer and to accelerate the convection liquid/vapor coefficient. These convection cells improve the evaporation process by inducing the thermal Marangoni number.

For this reason, **Table. 2** represent the lifetime of these cells during the evaporation process of the pure and gold-water mixture (5 and 10 nm) at 77 °C surface temperature.

The table has shown that the higher evaporation rate has a higher convection cell life and these results validate the increase in the evaporation rate of the 5nm Gold-water droplet.

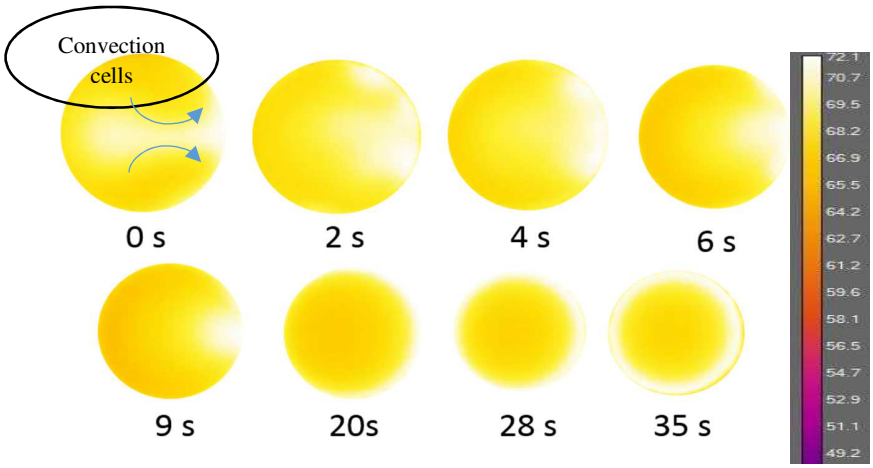

(a)

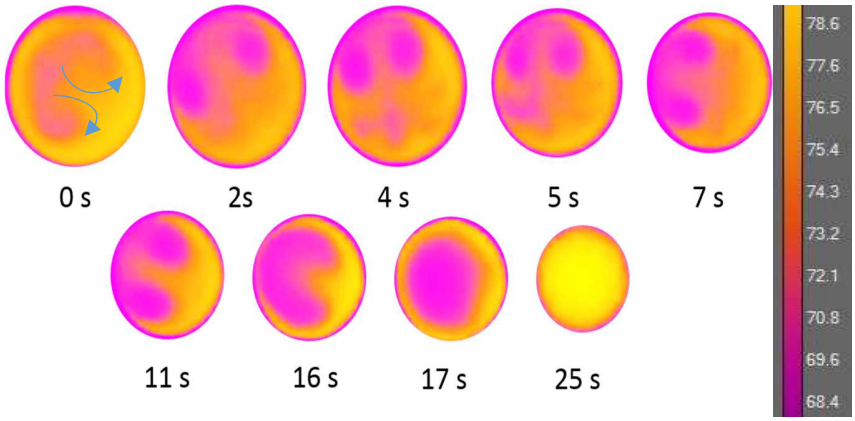

(b)

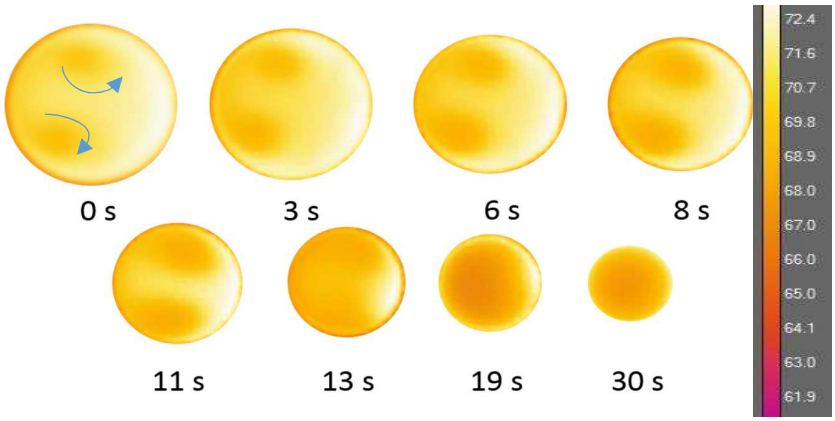

(c)

Figure 6. Snapshots from an infrared video of the evaporation process of (a) pure water (b) 5 nm Au-water and (c) 10 nm Au-water nanofluids at 50 % relative humidity and 77 °C surface temperature, 1%C_v.

Fluids/medium	**Convection cells lifetime (%)**
Water	5 %
5 nm Au-water,1% C_v	68 %
10 nm Au-water, 1% C_v	43 %

Table 2. Lifetime of the convection cells at 77 °C substrate temperature of pure water, 5 nm Au-water and 10 nm Au-water nanofluids.

3.1.2. Au nanofluid (1% C_v; Citrate-Capped- PBS solution) – Water Mixture, Citrate Effects.

The same measurements were made for the water-Au mixture of the same particle sizes (2.2, 5, 10 nm- Citrate-Capped- PBS solution) but with synthesis of the surface of gold nanoparticles with citrate in order to study the effect of citrate capping on enhancing the evaporation process. The result was compared to that of pure water on the $V^{2/3}$ plot. **Fig. 7** shows the evolution of $V^{2/3}$ for droplets of pure water and 1% C_v Au-water mixture of different particle sizes at different surface temperatures.

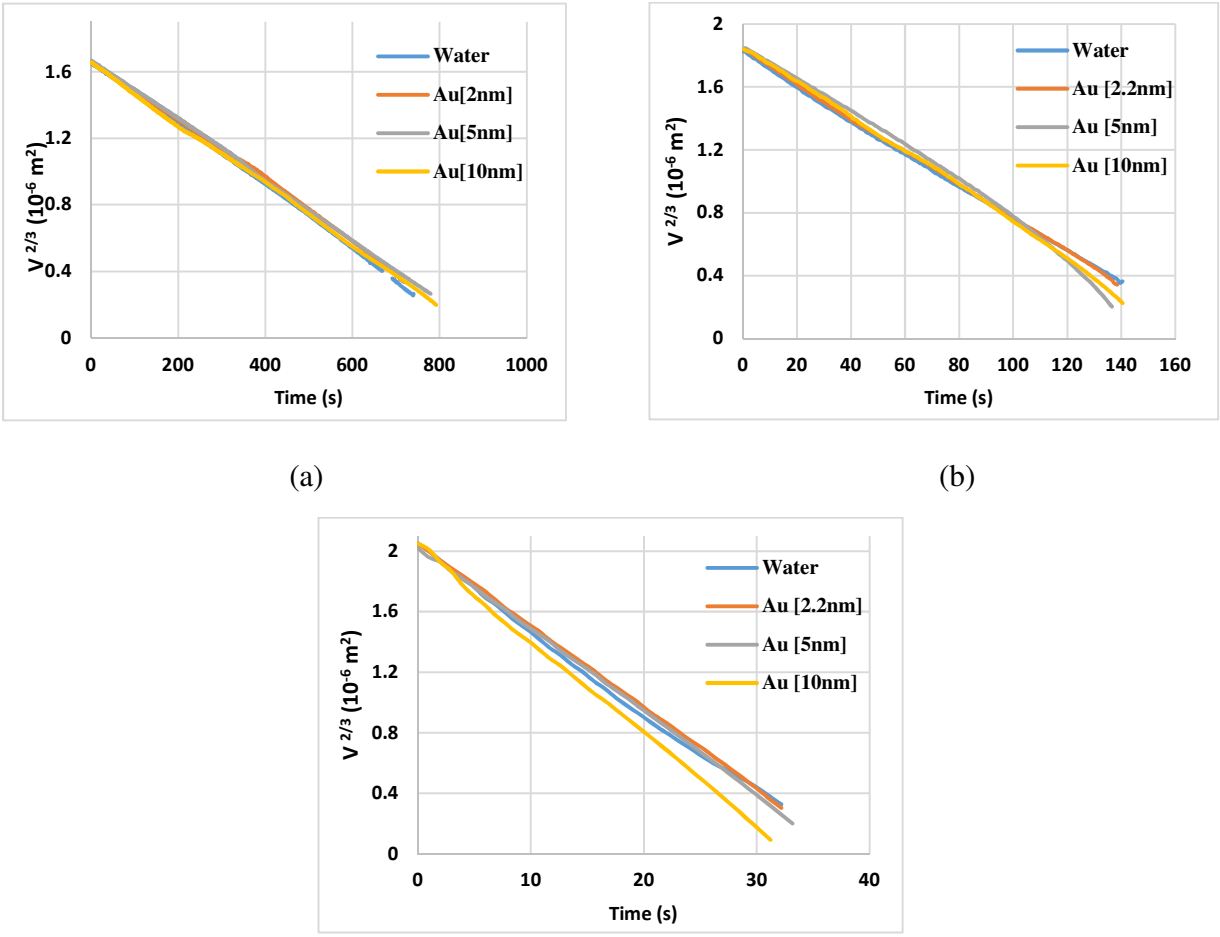

Figure 7. Evolutions of the volume for water and gold nanofluid (Citrate capping-PBS), with different particle sizes (2.2, 5 and 10 nm) under substrate temperatures (a) at ambient, (b) 55 °C and (c) 77 °C, versus time.

The results showed that at ambient temperature, the evaporation of pure water droplet was a little faster than the gold nanofluids of the three different sizes, with 2% more. When the surface temperature increased to 33 °C, the evaporation process showed a higher evaporation rate of the 10nm Gold-water mixture with 11% while 5% and 4% for the 2.2 and 5nm Gold-water mixtures respectively.

Similarly, at a surface temperature of 55 °C, the evaporation process showed a higher evaporation rate of the 10nm Gold-water mixture with 10% whereas 8% and 2% for the 2.2 and 5nm Gold-water mixtures respectively. Finally, the 10nm Gold-water mixture showed the

highest evaporation rate at the surface temperature of 77 °C with 15% more while 1% and 2% for the 2.2 and 5nm Gold-water mixtures respectively.

Thus, the evaporation rate, **Fig. 8**, was found to depend on the size of the nanoparticles, which showed that the largest particle size (10nm) has the greatest effect on increasing the evaporation proceeds during the droplet lifetime.

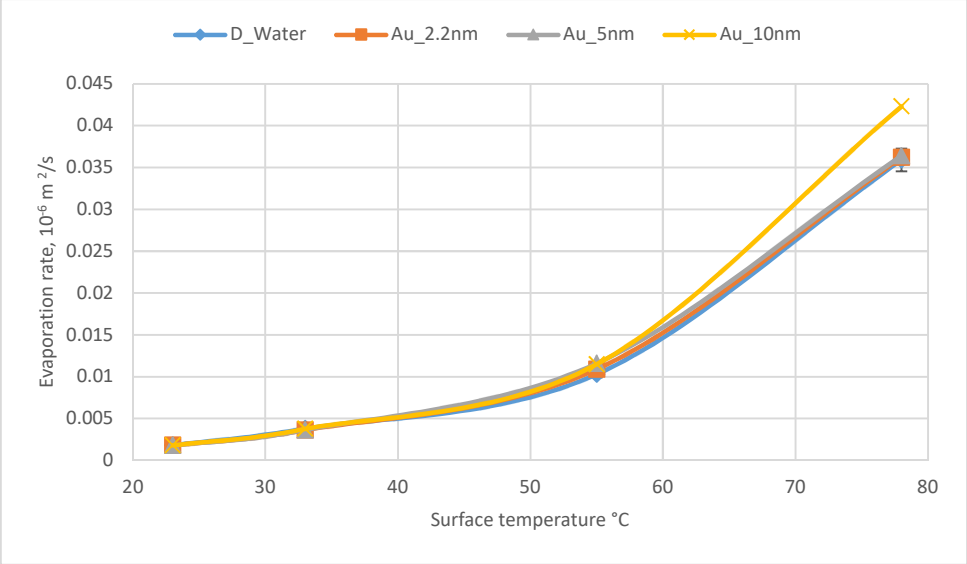

Figure 8. Evaporation rate of the citrated gold nanoparticle sizes at different surface temperatures

The Infrared Camera images made it possible to detect the convection cells, **Fig. 9,** due to the Marangoni effect that appeared on the surface of droplets. These convection cells have the ability to increase the vapor mass transfer at the liquid-air interfaces and to induce a faster evaporation rate [27]. But with citrate capping, no observation of Marangoni cells detected by the infrared camera. It showed a homogenization of the temperature profile. For this reason, the lifetime of these cells during the evaporation process was negligible.

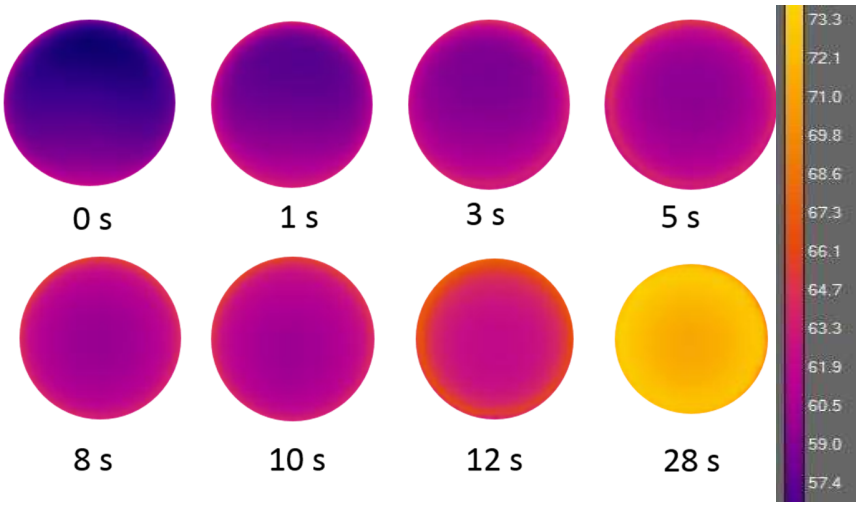

(a)

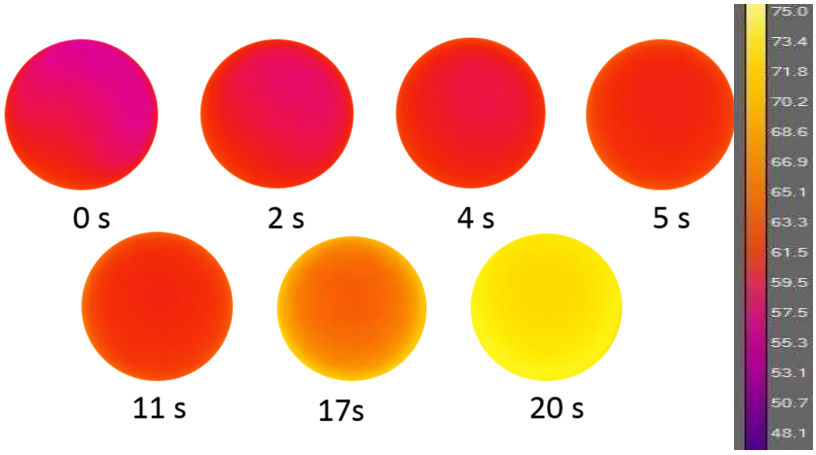

(b)

Figure 9. Snapshots from an infrared video of the evaporation process of (a) Citrated capping 5 nm Au-water and (b) Citrated capping 10 nm Au-water nanofluids at 50 % relative humidity and *77* °C surface temperature, 1%C_v

3.2. Acoustic investigations: Gold nanoparticles stability during droplet evaporation at ambient temperature.

Several precautions are taken to improve the accuracy of the measurements. The acoustic device is calibrated using water as a reference liquid, at ambient temperature. A drop of pure water is deposited on the hydrophobic silicon surface where the transducer (250 µm in diameter) is located. An acoustic wave (Longitudinal) is generated by the ZnO transducer through the substrate to the interface. The reflection coefficient of water is represented in **Fig. 10** during the evaporation process, demonstrates good reliability of the measured amplitude of the coefficient $|R| = 0.8594 \pm 0.01\%$.

This method makes it possible to follow the kinetics of the nanoparticle deposition. Drops of the same initial volume (1.5µL) are deposited, at ambient temperature, on the silicon substrate under controlled conditions (H=50%, T_{atm}=23°C). Various sizes of the gold nanoparticles (2.2, 5 and 10 nm) with and without citrate capping are then compared in order to analyze the stability of the nanoparticles during the evaporation process.

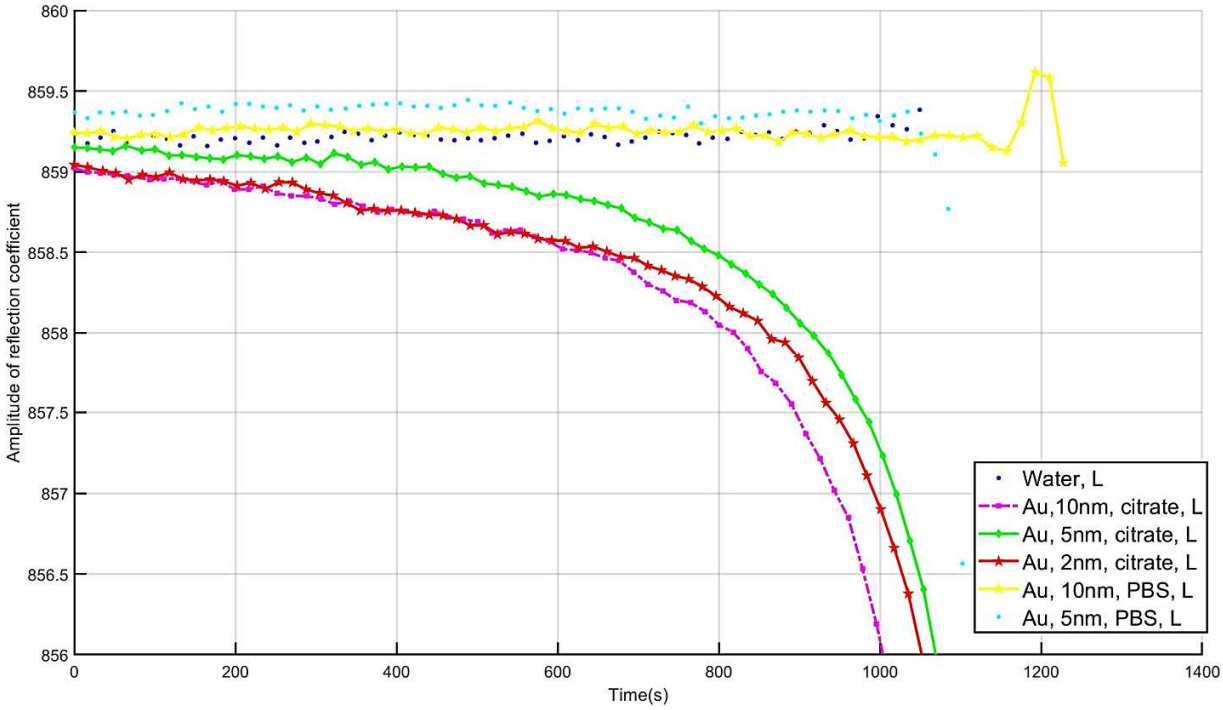

Figure 2. Reflection coefficient evolution of pure droplet (black), Au-PBS and Au-Citrate-PBS during evaporation process at 23°C.

In **Fig. 10**, the kinetics of the longitudinal reflection coefficient modulus for the different preparations, different sizes (2.2, 5 and 10 nm) and types of gold nanofluids (Citrate-capping PBS and PBS-reactant free), during the evaporation of a 4% C_v Gold-water mixture drop, are presented. One can notice a clear difference between the particles with and without citrate capping. Indeed, the reflection coefficient of the gold-water mixture drops with citrate capping (for all nanoparticle sizes) begins to decrease almost instantaneously until the end of the evaporation process. Whereas, for drops of the gold-water mixture without citrate (for all sizes of nanoparticles) the reflection coefficient showed a constant value and began to decrease at the end of the process. As discussed in [27], the variation of the reflection coefficient ascribed to a change of the physical properties of the material interacting with the ultrasounds at the interface. So, the change in the reflection coefficient is due to the gold nanoparticles deposition on the silicon substrate above the transducer.

Moreover, in the previous study [27], we have also shown that the sedimentation of the nanoparticle is correlated to the lifetime of Marangoni cells. Here, the Marangoni cells observed by an infrared camera, (*section 3.1)*, showed no convection cells for the coated gold nanoparticles, with citrate, during the evaporation process, this would, therefore, mean that the particles settle The acoustic method corroborates the link between dynamic deposition of nanoparticles and its effect on the lifetime of convection cells.

Fig. 11, present the final shape pattern of the evaporated Au-water droplets with and without citrate capping for all sizes, 2.2, 5 and 10 nm at ambient temperature. The change in the shape of the dried gold nanoparticles between citrate coated and non-coated nanoparticles are clearly observed. For the non-coated gold nanoparticles (with PBS), a normal and uniform coverage pattern can be observed whereas a viscoelastic pattern is observed for the citrate nanoparticles.

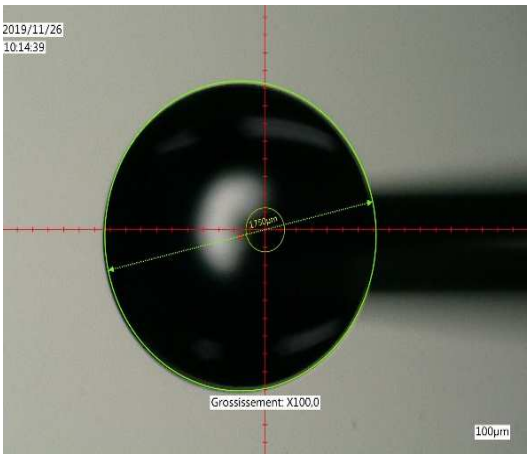
2019/11/26
10:14:39
1750µm
Grossissement: X100,0
100µm

(a)

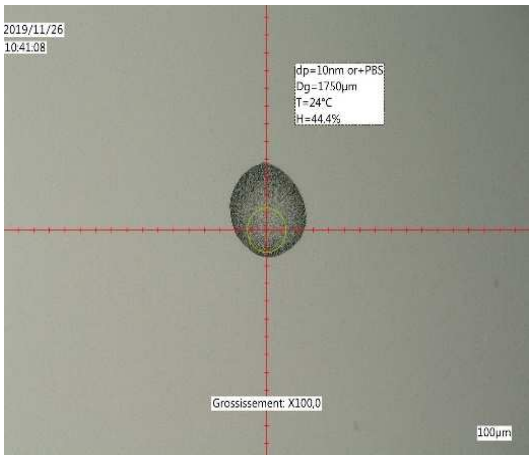
2019/11/26
10:41:08
dp=10nm or+PBS
Dg=1750µm
T=24°C
H=44.4%
Grossissement: X100,0
100µm

(b)

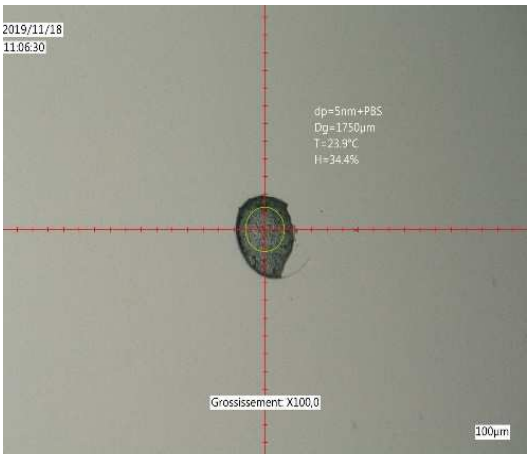
2019/11/18
11:06:30
dp=5nm+PBS
Dg=1750µm
T=23.9°C
H=34.4%
Grossissement: X100,0
100µm

(c)

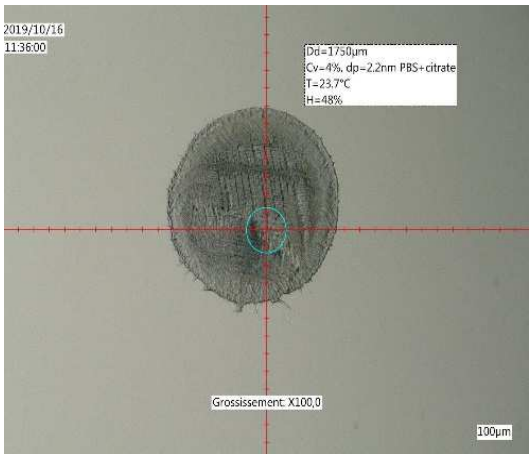
2019/10/16
11:36:00
Dd=1750µm
Cv=4%, dp=2.2nm PBS+citrate
T=23.7°C
H=48%
Grossissement: X100,0
100µm

(d)

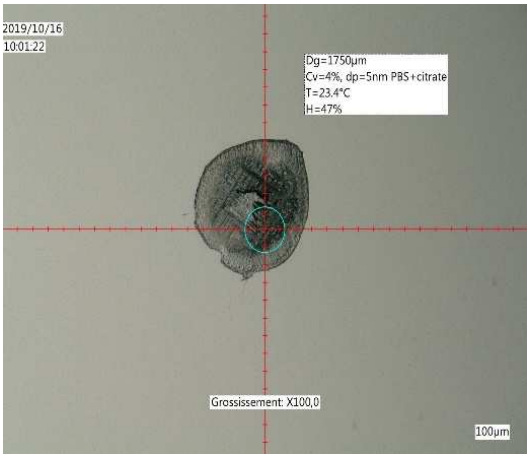
2019/10/16
10:01:22
Dg=1750µm
Cv=4%, dp=5nm PBS+citrate
T=23.4°C
H=47%
Grossissement: X100,0
100µm

(e)

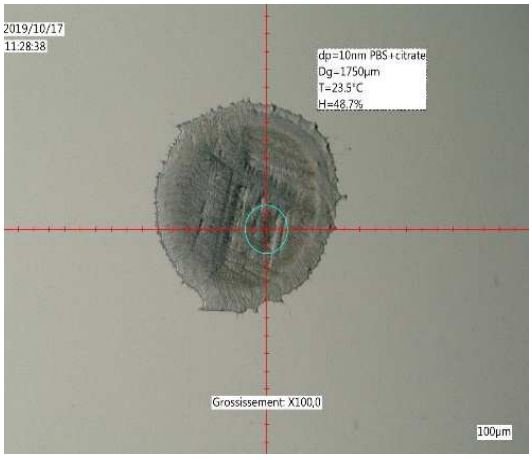
2019/10/17
11:28:38
dp=10nm PBS+citrate
Dg=1750µm
T=23.5°C
H=48.7%
Grossissement: X100,0
100µm

(f)

Figure 3. Gold Nanofluid Droplet deposited on silicon substrate and above the transducer (a) At starting point (b) Au-10nm- PBS (c) Au-5nm- PBS (d) Au-2.2nm-Citrate PBS (e) Au-5nm-Citrate PBS (f) Au-10nm-Citrate PBS (Nano particles Final shape pattern on the 250 µm transducer diameter)

In **Fig. 12**, a profilometer is used to measure the thickness of the deposited nanoparticles on the silicon substrate. Fig. 10.a, a thickness profile distribution of 5nm gold nanoparticles with PBS gives a mean value of 1.3 µm while 4.5 µm height for 5nm gold nanoparticles coated with citrate and PBS. This variation due to the high concentration of citrate in addition to PBS only.

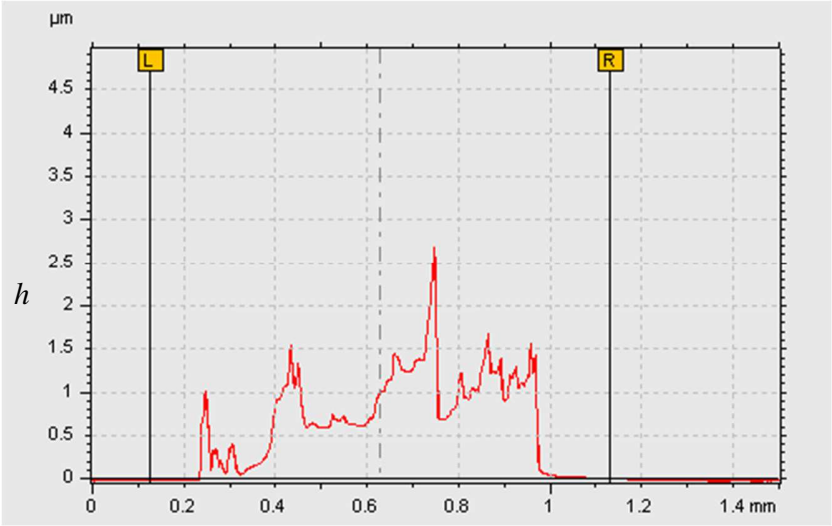

(a)

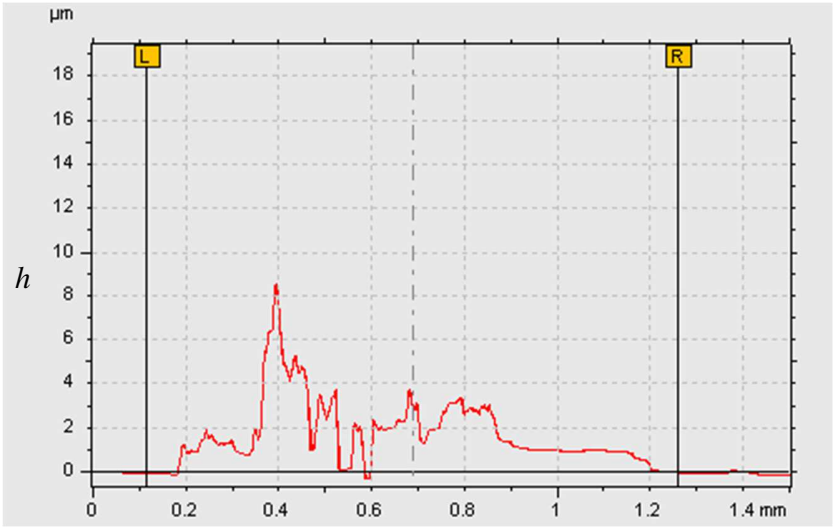

(b)

Figure 12. Thickness distribution of 5nm gold nanoparticles with 4% C*v*, (a) PBS solvent (b) Citrate coating with PBS solvent

These results are related to the infrared and optical. As explained previously, the evaporation rate of the gold nanoparticles with citrate-capping PBS was lower than that of gold nanoparticles with PBS-reactant free.

This can be explained, in addition to the thermal Marangoni effect, the importance of the stability of the nanoparticles inside the droplet has an important factor during its evaporation. Since the nanoparticles begin to settle early during evaporation process, this means that they will lose their effectiveness by absorbing the heat flux and to transporting it to the liquid-air interface.

4. Conclusion

The evaporation rate of gold Au-water nanofluid sessile droplets of 1% C_v has been measured in a controlled room temperature air (H=50%, T_{atm}=23 °C) using a Drop Shape Analyzer. The size effect of gold nanoparticle (2.2, 5 and 10 nm) was studied as well as different buffer solvents (Citrate-Capping PBS and no citrate-PBS) on the evaporation characteristics of droplets. The analysis was performed using two different methods, these methods have the ability to give a very important information on the fundamentals of droplet evaporation. An optical analysis, using Kruss system, was used to calculate the droplet evaporation rate of Au-water mixture at

different surface temperatures. While, an acoustic method represented by coefficient reflection waves has shown the ability to understand the deposition phenomenon of nanofluid at the solid/liquid interface. The main conclusion of this work are:

- The gold nanofluids droplets, for both solutions, evaporate more rapidly as the surface temperature increases in comparison to the evaporation of distilled water droplets.
- The uncapped gold nanofluids with PBS solution showed that the smallest nanoparticle size (5 nm) has the greatest impact on the evaporation rate (+35% more) than the larger nanoparticle, 10nm.
- The citrate-capped gold nanofluid showed opposite results, the larger nanoparticle (10nm) has the greatest improvement on evaporation rate (+15%) but still less than the solution with PBS only.
- The origin of the different behavior for the gold nanofluid compared to the pure water comes mainly from the thermophysical properties represented by thermal conductivity.
- The thermal Marangoni plays an important role on enhancing droplet evaporation. It showed that the convection cells were observed clearly and stayed longer for the 5nm uncapped gold nanoparticle (68%) compared to the 10nm (43%) from total evaporation time.
- No convection cells were observed for the citrate-capped gold nanofluid due to nanoparticles deposition. This behavior was proved using the high-frequency waves to the interface.
- This stability showed an important factor on droplet evaporation process.

Author Information

Corresponding Author

*Email: souad.harmand@uphf.fr

Ibrahim.zaaroura@hotmail.com

Acknowledgments

The authors would like to acknowledge the financial support from the Jeumont Electric, CE2I-CPER, Renatech, French state and Region ‘Hauts de France’ for this work.

Annex A

1- Volume and wetting base diameter evolutions during droplets evaporation of pure water and uncapped gold nanofluid-PBS (5 and 10 nm).

a- 5 nm gold nanoparticle

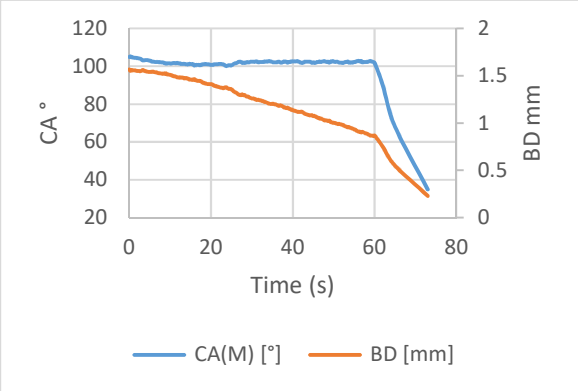

(b) T_s = 55 °C

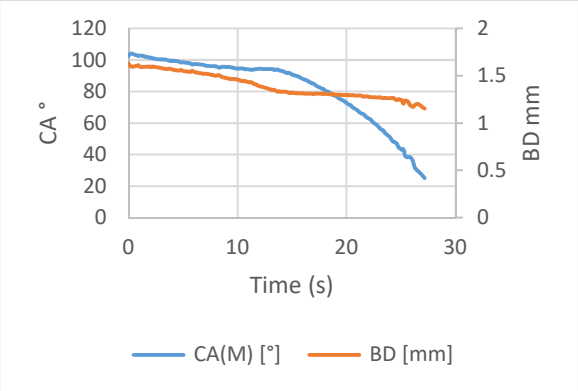

(a) T_s = 77 °C T_s

b- 10 nm gold nanoparticle

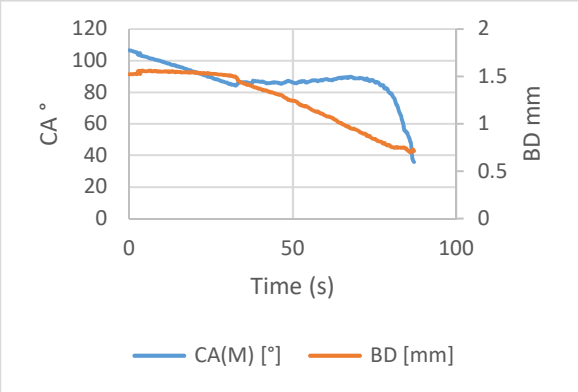

(a) T_s = 55 °C

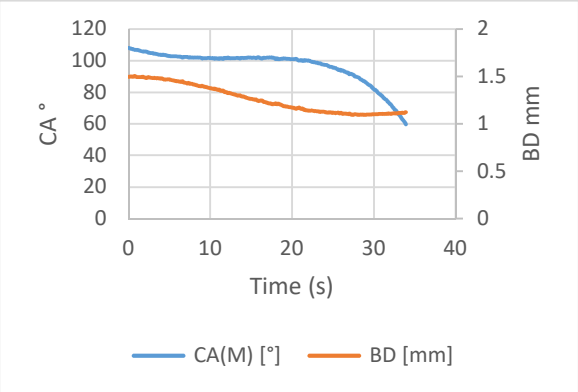

(b) T_s = 77 °C

c- Water droplet

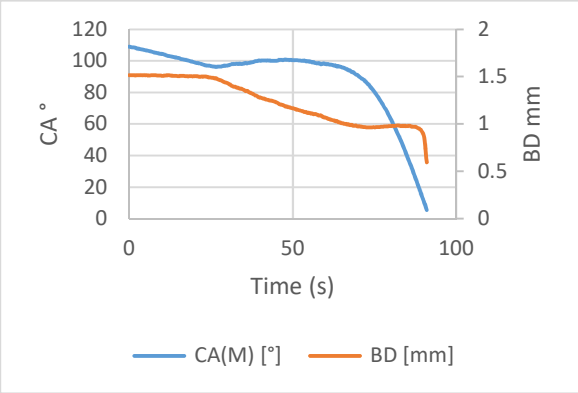

(a) T_s = 55 °C

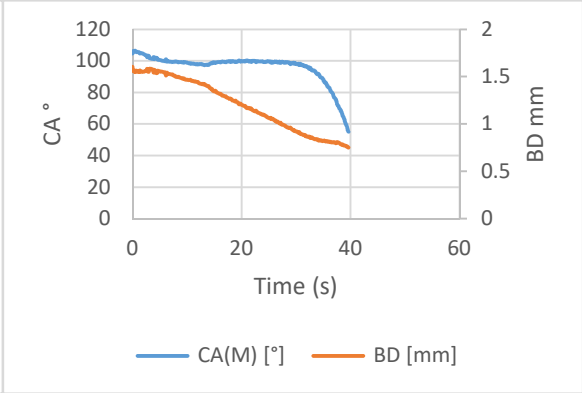

(b) T_s = 77 °C

2- Volume and wetting base diameter evolutions during droplets evaporation of pure water and citrate-capped gold nanofluid-PBS (5 and 10 nm).

a- Pure water

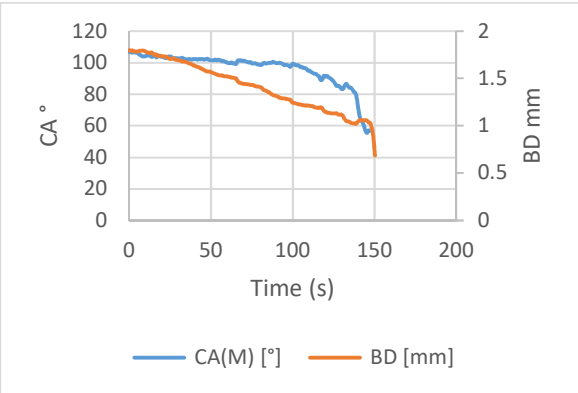

(b) T_s = 55 °C

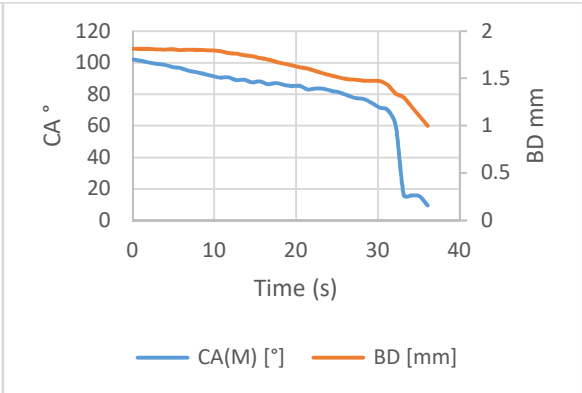

(a) T_s = 77 °C

b- 2 nm gold nanoparticle

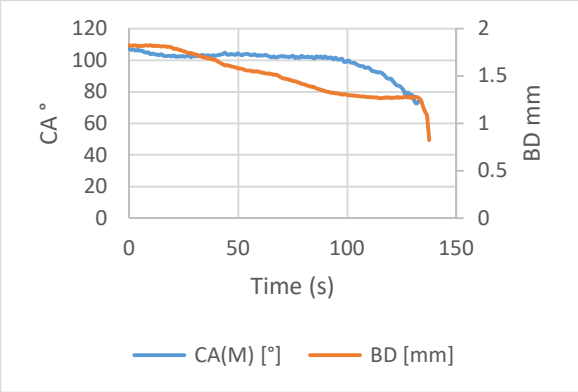

(a) T_s = 55 °C

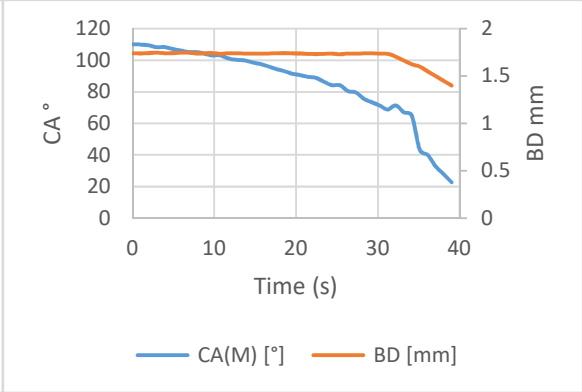

(b) T_s = 77 °C

c- 5 nm gold nanoparticle

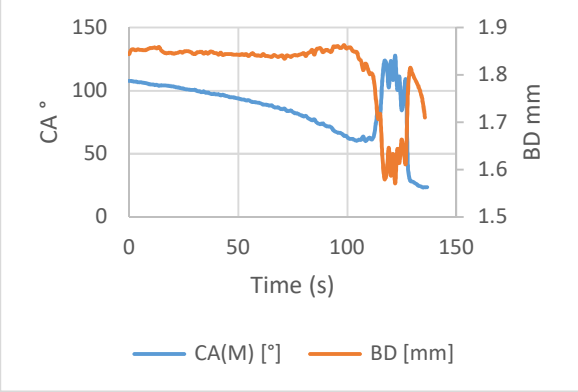

(a) T_s = 55 °C

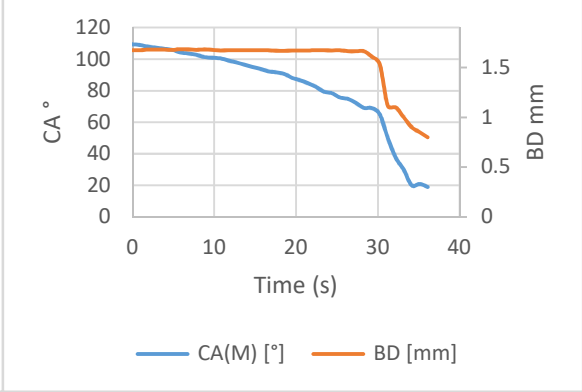

(b) T_s = 77 °C

d- 10 nm gold nanoparticle

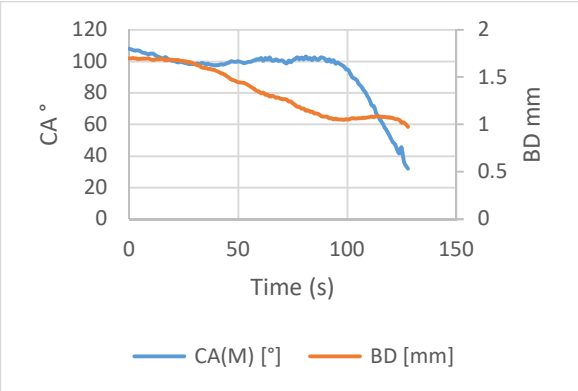

(a) T_s = 55 °C

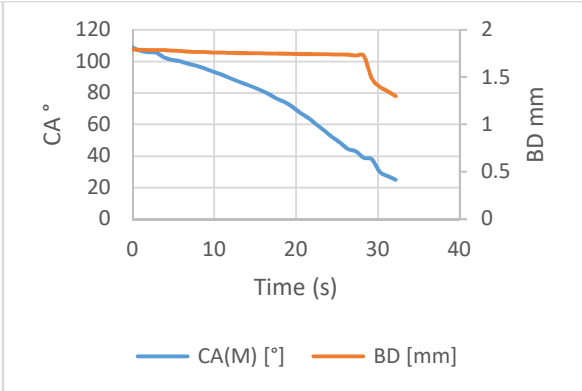

(b) T_s = 77 °C

Annex B

Repeatability at 77 °C surface temperature.

1- Pure water

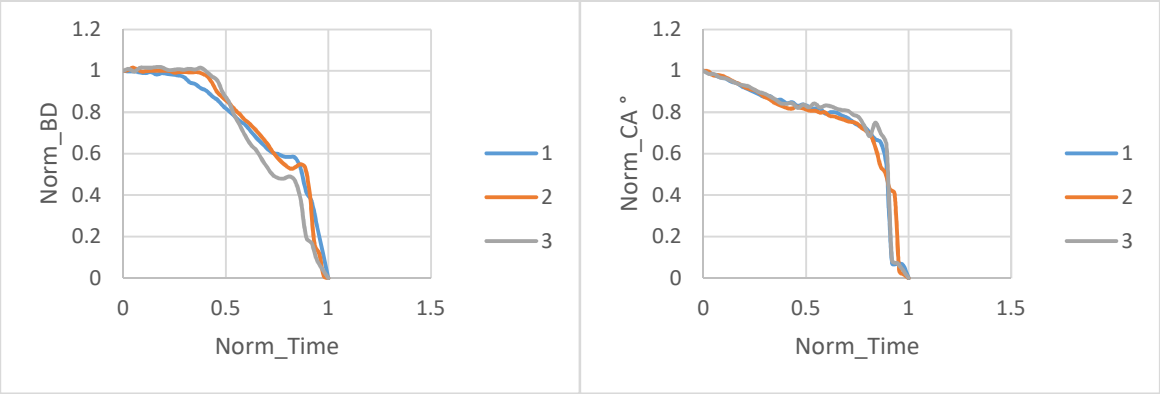

Figure 13. The repeatability of the Contact angle and base diameter variations of pure water droplet at 77 °C surface temperature.

2- 2 nm Citrate-PBS gold nanofluid.

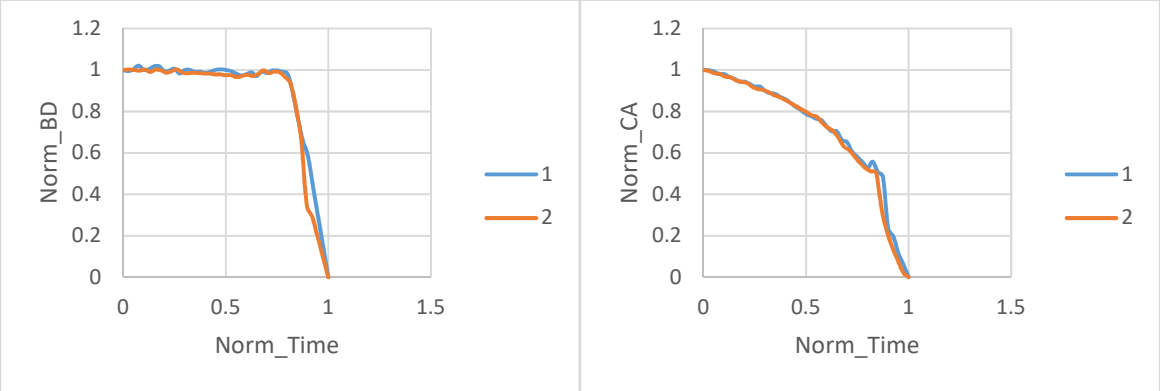

Figure 14. The repeatability of the contact angle and base diameter variations of 2nm citrate-PBS gold/ water droplet at 77 °C surface temperature.

3- 5 nm Citrate-PBS gold nanofluid.

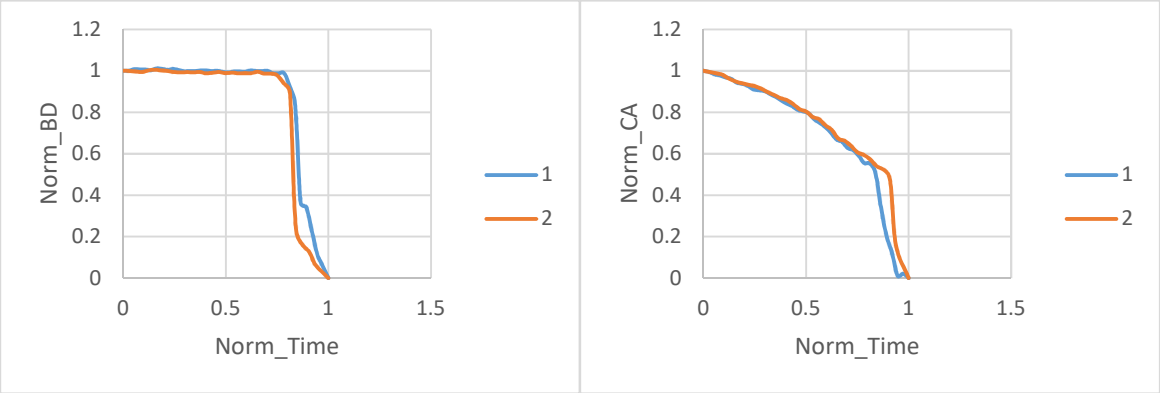

Figure 15. The repeatability of the contact angle and base diameter variations of 5nm citrate-PBS gold/ water droplet at 77 °C surface temperature.

4- 10 nm Citrate-PBS gold nanofluid.

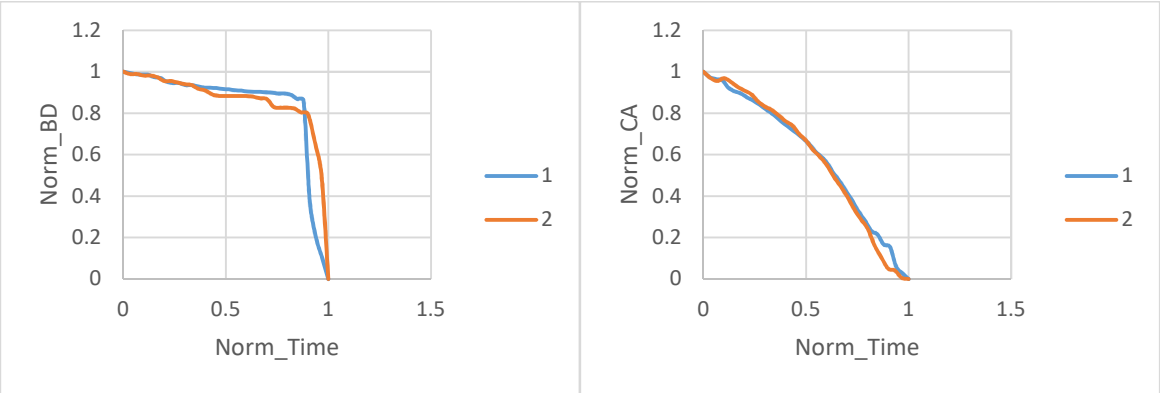

Figure 16. The repeatability of the contact angle and base diameter variations of 10nm citrate-PBS gold/ water droplet at 77 °C surface temperature.

References

[1] C. T. Nguyen, G. Roy, C. Gauthier, N. Galanis, Heat transfer enhancement using Al_2O_3-water nanofluid for an electronic liquid cooling system, Appl. Therm. Eng, 27 (2006), 1501-1506.

[2] P. Imani Mofrad, S. Zeinali Heris, M. Shanbedi, Experimental investigation of the effect of different nanofluids on the thermal performance of a wet cooling tower using a new method for equalization of ambient conditions, Energy Convers Manage, 158 (2018), 23-35.

[3] M. Rafati, A.A. Hamidi, M.S. Niaser, Application of nanofluids in computer cooling systems (Heat transfer performance of nanofluids), Appl. Therm. Eng, 45(46), (2012) 9-14.

[4] S. Jafarmadar, N. Azizinia, N. Razmara, F. Mobadersani, Thermal analysis and entropy generation of pulsating heat pipes using nanofluids, Appl. Therm. Eng, 103 (2016) 356-364.

[5] U. Choi, Enhancing thermal conductivity of fluids with nanoparticles, ASME Fluid Eng. Div. 231 (1995) 99–105.

[6] N. S. Akbar, M. Raza, R. Ellahi, Copper oxide nanoparticles analysis with water as base fluid for peristaltic flow in permeable tube with heat transfer, Computer Methods and Programs in Biomedicine, 130 (2016) 22-30.

[7] M. P. Beck, T. Sun, A. S. Teja, The thermal conductivity of alumina nanoparticles dispersed in ethylene glycol, Fluid Phase Equilibria, 260 (2007), 275-278.

[8] S. Simpson, A. Schelfhout, C. Golden, S. Vafaei, Nanofluid thermal Conductivity and Effect Parameters, Appli. Sci, 9(1) (2019) 87.

[9] M. Karimzadehkhouei, M. Shojaeian, K. Sendur, M.P. Menguc, A. Kosar, The effect of nanoparticles type and nanoparticle mass fraction on heat transfer enhancement in pool boiling, Int. J. Heat Mass Transfer 109 (2017) 157-166.

[10] Y. Xuan, Q. Li, Heat transfer enhancement of nanofluids, Int. J. Heat Fluid Flow 21 (2000) 58-64.

[11] L. Dongliang, P. Hao, L. Deqing, Thermal Conductivity Enhancement of Clathrate Hydrate with Nanoparticles, Int. J. Heat Mass Transfer 104 **(2017)** 566-573.

[12] E. Abu-Nada, Effects of variable viscosity and thermal conductivity of Al_2O_3-water nanofluid on heat transfer enhancement in natural convection, International Journal of Heat and Fluid Flow, 30 (2009), 679-690.

[13] M. Ghanbarpour, E.B. Haghigi, R. Khodabandeh, Thermal properties and rheological behavior of water based Al_2O_3 nanofluid as a heat transfer fluid, Experimental Thermal and Fluid Science, 53 (2014), 227-235.

[14] Y. Ding, H. Alias, D. Wen, R. A. Williams, Heat transfer of aqueous suspensions of carbon nanotubes (CNT nanofluids), Int. J. Heat Mass Transfer, 49 (2006), 240-250

[15] N. Sandeep, A. Malvandi, Enhanced heat transfer in liquid thin film flow of non-Newtonian nanofluids embedded with graphene nanoparticles, Advanced Powder Technology, 27 (2016), 2448-2456.

[16] R. Manimaran, K. Palaniradja, N. Alagumurthi, S. Sendhilnathan, J. Hussain, Preparation and characterization of copper oxide nanofluid for heat transfer applications, Applied Nanoscience, 4 (2014), 163-167.

[17] P. Warrier, A. Teja, Effect of particle size on the thermal conductivity of nanofluids containing metallic nanoparticles, Nanoscale Research Letters, 6 (2011) 247.

[18] M. H.U. Bhuiyan, R. Saidur, M.A. Amalina, R.M. Mostafizur, A. Islam, Effect of nanoparticles concentration and their size on surface tension of nanofluids, Procedia Engineering 105 (2015), 431-437.

[19] S. Yao, X. Huang, Y. Song, Y. Shen, S. Zhang, Effects of nanoparticles types and size on boiling feat transfer performance under different pressures, AIP advances, 8, 025005 (2018).

[20] S. Tanvir, S. Biswas, L. Qiao, Evaporation Characteristics of Ethanol Droplets Containing Graphite Nanoparticles Under Infrared Radiation, Int. J. Heat Mass Transfer 114 (2017) 541-549.

[21] N. Grich, W. Foudhil, S. Harmand, S. Ben Jabrallah, Experimental study of the effect of water spray in the air on thermal transfer along a plate of an exchanger, J. heat transfer, (2020).

[22] Y. Chan Kim, Evaporation of nanofluid droplet on heated surface, Adv. Mech. Eng, 7 (4) (2015) https://doi.org/10.1177/1687814015578358

[23] K. Sefiane, R. Bennacer, Nanofluids droplets evaporation kinetics and wetting dynamics on rough heated substrate, Adv. Colloid Interface Sci., 147-148 (2009) 263-271.

[24] J. T. Cieslinski, K. A. Krygier, Sessile droplet contact angle of water-Al_2O_3, water-TiO_2 and water-Cu nanofluids, Exp. Therm. Fluid Sci., 59 (2014) 258-263.

[25] X. Zhong, A. Crivoi, F. Duan, Sessile nanofluid droplet drying, Adv. Colloid Interface Sci., 217 (2015) 13-30.

[26] P. Chen, S. Harmand, S. Szunerits, R. Boukherroub, Evaporation behavior of PEGylated graphene oxide nanofluid droplets on heated substrate, Int. J. Thermal Sciences, 135 (2019) , 445-458.

[27] I. Zaaroura, M.Toubal, H. Reda, J. Carlier, S. Harmand, R. Boukherroub, A. Fasquelle, B. Nongaillard "Evaporation of nanofluid sessile drops: Infrared and acoustic methods to track the dynamic deposition of copper oxide nanoparticles", Int. J. Heat Mass Transfer 127, Part B (2018) 1168-1177.

[28] H. Hu, R. G. Larson, Marangoni effect reverses coffee-ring depositions, J. Phys. Chem. B 110 (2006) 7090-7094.

[29] H. Hu and R. G. Larson, Analysis of the effects of Marangoni stresses on the microflow in an evaporating sessile droplet, Langmuir, 21 (2005) 3972-3980.

[30] A. M. Benselama, S. Hramand, K. Sefiane, Thermocapillary effects on steadily evaporating contact line: A perturbative local analysis, Physics of Fluids, 24 (2012) 072105.

[31] S. Breisch, B.D. Heij, M. Lohr, M. Stelzle, Selective Chemical Surface Modification of Fluidic Microsystems and Characterization Studies, J. Micromech. Microeng. 14 **(2004)** 497-505.

[32] S. Li, J. Carlier, M. Toubal, H. Liu, P. Campistron, D. Callens; G. Nassar, B. Nongaillard, S. Guo, High Frequency Acoustic on-Chip Integration for Particle Characterization and Manipulation in Microfluidics. Appl. Phys. Lett. 111 (2017) 163503.

[33] S. Chandra, M. di Marzo, Y. M. Qiao and P. Tartarini, Effect of Liquid-Solid Angle on Droplet Evaporation, Fire Safty Journal 27 (1996) 141-158.

[34] P. Chen, S. Harmand, S. Ouenzerfi, J. Schiffler, Marangoni Flow Induced Evaporation Enhancement on Binary Sessile Drops, J. Phys. Chem, B, 121(23) (2017) 5824-5834.